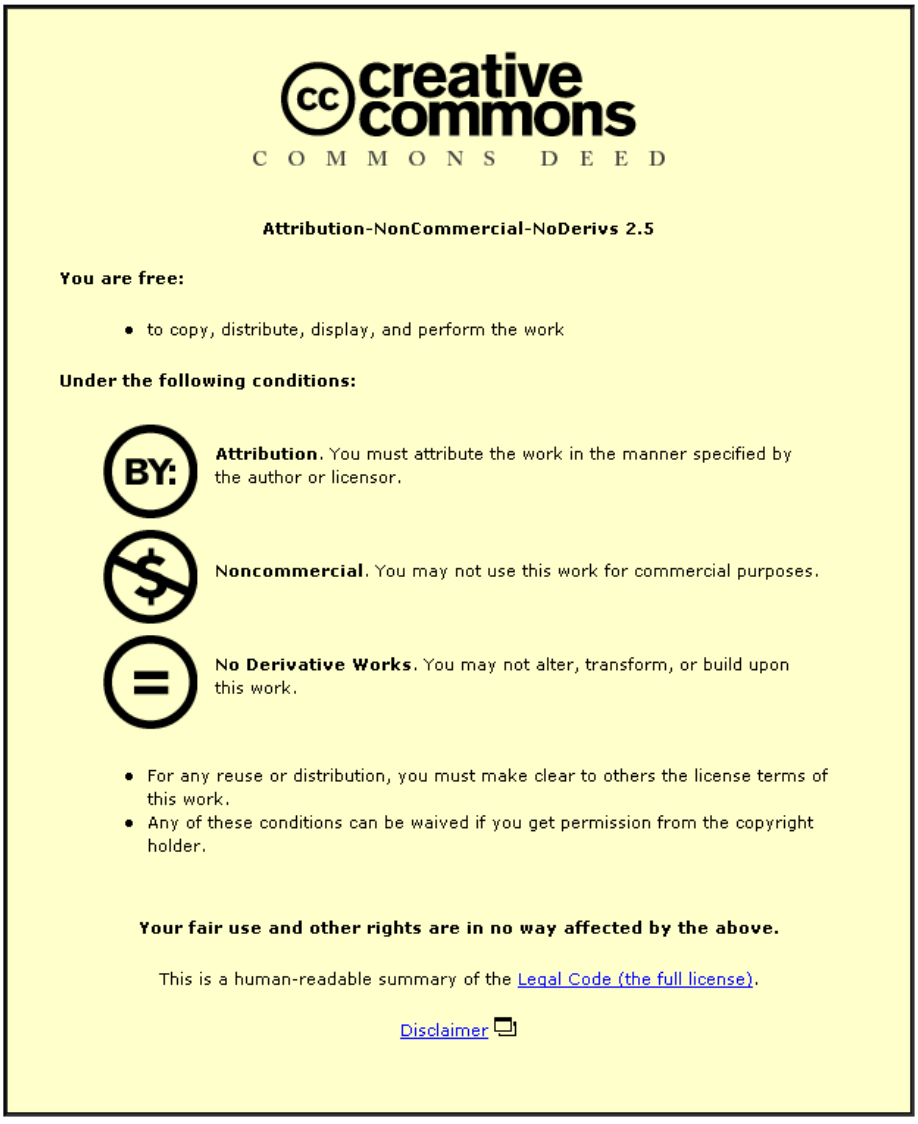

creative commons

COMMONS DEED

Attribution-NonCommercial-NoDerivs 2.5

You are free:

- to copy, distribute, display, and perform the work

Under the following conditions:

Attribution. You must attribute the work in the manner specified by the author or licensor.

Noncommercial. You may not use this work for commercial purposes.

No Derivative Works. You may not alter, transform, or build upon this work.

- For any reuse or distribution, you must make clear to others the license terms of this work.
- Any of these conditions can be waived if you get permission from the copyright holder.

Your fair use and other rights are in no way affected by the above.

This is a human-readable summary of the Legal Code (the full license).

Disclaimer

NPL

NPL REPORT ENG 34

The use of areal surface texture parameters to characterize the mechanical bond strength of copper on glass plating applications

He, B, Petzing, J, Webb, P, Conway, P, Leach, R K

JANUARY 2012

The use of areal surface texture parameters to characterize the mechanical bond strength of copper on glass plating applications

Baofeng He, Jon Petzing, Paul Conway
Wolfson School of Mechanical & Manufacturing Engineering
Loughborough University

Patrick Webb
The Manufacturing Technology Centre
Coventry

Richard Leach
Engineering Measurement
National Physical Laboratory

ABSTRACT

This report describes research into the role that surface topography plays in influencing the mechanical bond strength of the electroless copper plating of novel glass substrates. The work considers bespoke laser machining of glass substrates, electroless plating chemistry, areal surface topography analysis using non-contact optical techniques, paramaterization of the surfaces using areal parameters described in ISO 25178, and scratch testing of plated copper to measure the adhesive bond strength. By correlating bond strength to appropriate areal parameters, it is anticipated that better mechanical adhesive potential of machined glass surfaces can be achieved.

ISSN: 1754-2987

National Physical Laboratory
Hampton Road, Teddington, Middlesex, TW11 0LW

Approved on behalf of NPLML by Dr Andrew Lewis, Assistant Knowledge Leader.

Contents

List of figures

List of figures

1 INTRODUCTION AND BACKGROUND

The research presented here starts to evaluate the role that surface topography may have on influencing the mechanical bond strength of the electroless copper plating process. The central aims of the research are to:

- improve mechanical adhesion of copper on glass, thus improving electronic functionality and life cycle; and

- correlate adhesion quality with areal surface texture parameters to identify parameters that can reduce the design/testing cycle of glass surface preparation and acceptance.

The drive towards increasing densities of components and integrated circuit inputs/outputs in electronics is pushing the capabilities of conventional printed circuit board (PCB) manufacture to its limits. Whilst sub-100 μm metal features can be produced, the dimensional instability of organic material-based boards in response to changes in temperature or humidity means such features cannot be reliably aligned. Glass is attractive as an alternative substrate material due to its relatively low cost and has high thermal stability, with a coefficient of thermal expansion similar to that of silicon. Glass has the added benefit that it is transparent, which could simplify assembly and inspection of components with area array or hidden interconnects, and facilitate developments in optoelectronic circuitry with optical interconnects.

The concept of using glass for high density interconnects has been explored by several research groups [1]. Previous work at Loughborough University (LU) has examined the feasibility of the major process steps required to form a high density, multilayer glass circuit board; glass layer lamination, drilling of microvias, and electrical interconnect pattern formation [2-6]. The method chosen for the latter was electroless plating of copper due to its process advantages over other alternatives, such as reduced energy consumption and cost, and enhanced deposition rate. It was possible to plate layers up to 150 nm in thickness with good adhesion when using a silane adhesion promotion coating, however thicker layers tended to peel off.

A further measure to improve plating adhesion would be to texture the glass surface. In the previous work randomly rough surfaces showed improved plating retention compared to smooth untreated glass, although systematic understanding the influence of surface texture was not previously a research priority. However, it seems likely that controlling the surface texture would improve adhesion still further, potentially allowing mechanical enhancement to the bond strength between plated metals (such as copper) and glass substrates, in addition to the traditionally considered electrochemical bonding characteristics.

Whilst previous researchers have reported that micro-columnar array structures could enhance adhesive bonding strength for metals and alloys [7-9], there has been little progress in generating micro-scale patterned structures on glass. Techniques have, therefore, been developed at LU to produce a variety of textures and structures on glass substrates, allowing a systematic study of the effect of surface texture on electroless plated copper adhesion. This has primarily involved the use of excimer laser machining technology to selectively ablate small areas of glass.

Many modern surface measurement instruments are capable of capturing a surface map of height data, rather than simply a 2D profile more typically produced by a contact stylus. If a traditional profile-based surface parameter such as *Ra* is then calculated [10], only a small fraction of the data collected is used. Areal parameters by contrast make full use of the 3D data set [11], and in principle capture much more of the complexity of surfaces. Increased data density and use may be important, for example, if the interaction of the stress state of the plated layer on the glass with protruding micro-scale features of the surface, plays a role in enhancing adhesion.

The literature on the analysis and applications of areal surface topography over the last twenty years covers a diverse range of disciplines, including; manufacturing, materials, optics and biology. Examples of industrial applications of areal surface analysis related to the functional features are listed in Appendix 1 [12-30]. These industrial application examples demonstrate a breadth of surface texture parameter identification. However, it is noted that a significant proportion of the cited literature does not link understanding of the influence of each parameter to the surface properties or functionality, or necessarily provide explanations for the original choices of parameter. Furthermore, the majority of researchers have not used areal parameters for describing surfaces for adhesive bond quality.

The complex relationship between surface texture and adhesion has interested scientists and engineers for more than fifty years. Examples of research output are identified in Appendix 2 [31-44], where authors identify that varying degrees and types of surface texture appear to have beneficial effects on adhesion. Analysis of these examples indicates that surface topography is typically considered in a superficial manner. Furthermore, although surface profile parameters may potentially be restrictive and misleading, very few adhesion researchers have considered areal surface texture parameters to characterize surface texture over the last ten years, a period of time within which equipment, data processing software and published texts have provided access to the use of areal parameters. Whilst an example of the use of the *Sa* parameter can be cited in the context of adhesion [36], little attempt has been made to consider the breadth of parameters (and consequently surface description) available. It can also be identified that no evidence can be found of publications concerning bespoke texturing of glass for electroless copper plating.

The lack of a body of knowledge concerning the use of areal parameters for adhesion, and specifically electroless copper coating of glass, is both a hindrance (*i.e.*, a lack of published research direction) but also an opportunity for this current research to demonstrate unique and novel findings. In this report the development of the experimental techniques used is described, initial results obtained and analysis are presented and discussed, with reference to chosen areal parameters. The novelty of the work reported here is in identifying and producing the optimal surface topography for adhesion of plated metal layers on glass, and linking this to areal parameters that describe the surfaces. It should also be noted that the manufacturing techniques used within this research are not proposed as production methods for future glass based PCBs, but have been chosen for their versatility and controllability within the context of experimental investigation.

2 RESEARCH AIMS AND OBJECTIVES

The research presented here starts to question the role that surface topography may have on influencing the mechanical bond strength of the electroless copper plating. The aims of the research are to:

- improve mechanical copper adhesion on glass, thus improving electronic functionality and life cycle; and
- correlate adhesion quality with 3D/areal parameters to identify parameters that can reduce the design/testing cycle of glass surface preparation/acceptance.

The following objectives are identified as key measures of project progress.

- Investigate manufacturing processes for the machining of micrometre scale features into glass substrates.
- Investigate manufacturing processes for producing (controlled) randomly rough surfaces on glass substrates.
- Develop contact/non-contact metrology techniques to routinely measure micrometre scale features on glass substrates.
- Assimilate and develop copper plating chemistry for textured glass surfaces.
- Develop and apply quantifiable scratch testing techniques for assessing copper/glass bond strength (critical load) using NPL-based equipment.
- Produce a number of glass batches with sequentially refined surfaces, and test at NPL.
- Produce statistics that demonstrate the quality of correlation between critical load values (adhesive bond strength) and a range of ISO 25178 areal parameters.
- Identify key ISO 25178 areal parameters that provide routinely robust characterization of glass textured surfaces that are identified as being suitable for electroless copper plating and enhanced cooper bond strength.

3 PROCESSING AND MEASUREMENT OF GLASS

A range of methods and techniques for the production of textured glass surfaces has been considered during this research, and can be categorized into the production of randomly rough surfaces and the production of structured surfaces.

- The production of randomly rough surface preparation has been investigated and the following techniques considered: acid etch, bead blasting, micro-sand blasting and plasma etching, all of which produce randomly rough surfaces, but with limited control over volume of material removal per unit area, and subsequent roughness values.

- The preparation of structured surfaces has been investigated and the following techniques considered: mechanical machining and laser machining. Laser machining (or ablation) provides finesse of material removal that mechanical machining struggles to match, unless diamond turning techniques are used.

The research needed to initially address the ability to produce glass surfaces with the maximum amount of control, repeatability and material removal finesse. These criteria maximize the opportunity to study cause and effect, in terms of glass surface mechanical structure (characterized *via* areal parameters) and copper adhesion quality. The requirement to eventually consider volume or large scale manufacturing can then be subsequently addressed in terms of process change to optimize lead time and cost reduction. To this end, the majority of glass surface preparation has used excimer laser machining (ablation) [45, 46].

3.1 LASER MATERIALS PROCESSING

Cerium doped glass (CMG specification) supplied by Qioptiq Ltd was chosen as a substrate material due to the beneficial absorption characteristics at the excimer laser wavelength available (248 nm) thus maximizing glass removal efficiency, and the similarity of thermal expansion coefficient to silicon. The glass sheets were supplied as square samples with lateral dimensions of 40 mm × 40 mm, and thicknesses of 100 μm and 500 μm.

A krypton fluoride (KrF) excimer laser (model EMG 203, Lambda Physik) operating at 248 nm was used for machining the CMG glass. The laser system parameters, including output pulse energy (200 mJ to 250 mJ), repetition rate (5 Hz to 25 Hz), and shots per area (5 to 200), were varied and optimized according to the surface topography and adhesion performance of the samples. Various metal masks with square, circular and triangular apertures were placed in the laser path to tailor the size and the shape of laser beam projected onto the glass work substrates. The excimer laser was typically operated at energy density of 26 $mJ\,mm^{-2}$ and a pulse frequency of 10 Hz.

Excimer lasers can generate micro-scale pattern array structures on glass by using a mask projection and dragging process [45,46]. Complex micro-scale structures were typically produced in two steps. Firstly, the work piece (glass) was mounted on the computer numerically controlled (CNC) work stage to form a groove contour along one direction, with step-wise repetition of the process forming overlapping grooves. Secondly, (and where necessary) grooves were machined orthogonally to the initially machined grooves, creating segmented periodic structures.

A range of novel and complex micro-scale patterned structures of various depths were generated on CMG glass by changing the mask geometry, mask dimensions and laser operation parameters. Laser variables were investigated systematically to minimize the micro-roughness effect during production of the structured surfaces, micro-roughness being an inherent function of the fluctuating spatial energy density of the laser beam profile.

3.2 BASIC METHODOLOGY

The basic methodology and techniques used to correlate surface topography with adhesion performance are shown in figure 1, and can be summarized as:

- excimer laser machining with control of machining variables;
- application of contact/non-contact surface metrology to characterize the machined surfaces prior to coating via areal parameters;
- electroless copper plating with control of plating variables;
- scratch testing of copper plating to identify critical load of failure (adhesive bond failure); and
- correlation of failure critical loads versus areal parameter values.

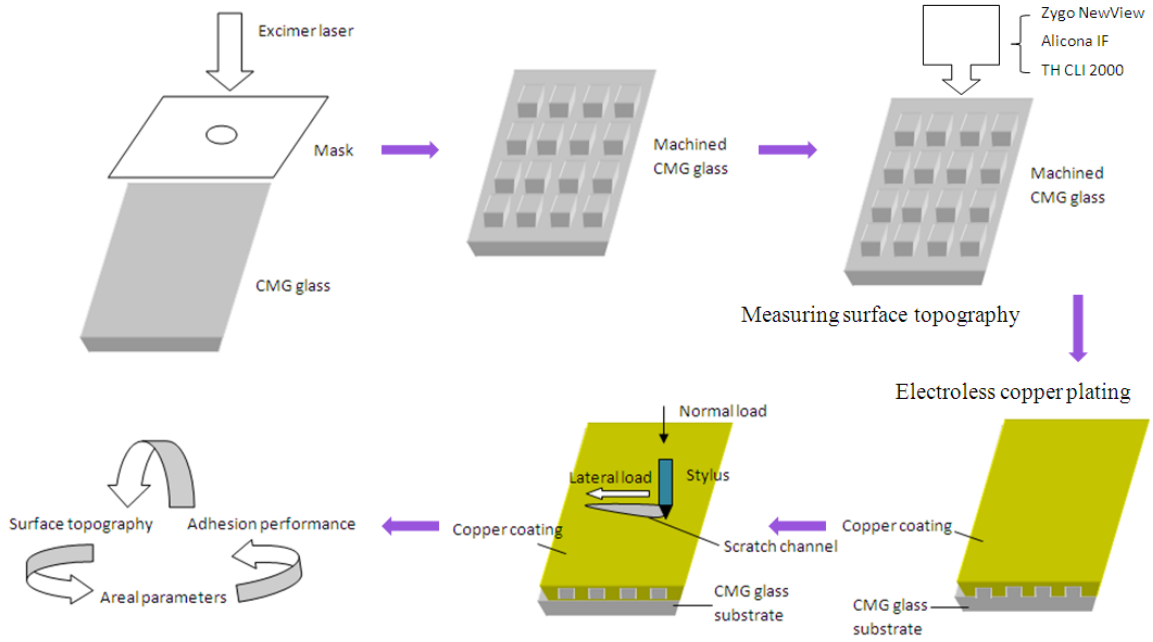

Figure 1. Basic methodologies and techniques

The surface topographies were characterized using non-contact areal surface topography measurement techniques such as coherence scanning interferometry (CSI) [47] and focus variation (FV) [48, 49], coupled with the new ISO 25178-2 areal surface texture parameters [11]. Typically a 10× lens was used on each instrument, providing a lateral field of view of approximately 700 µm × 500 µm.

A Zygo NewView 5000 CSI system was predominantly employed to measure the majority of the surface topographies of each machined micro-pattern. Typical areal surface topography images machined by different masks are shown in figure 2 and figure 3. These images show novel grid pattern micro-structures on the CMG glass surfaces produced by using circular and square masks. Micro-ramp and pyramid pattern structures can be produced by using triangular masks. When using fixed mask and laser parameter settings, the topography of the micro-pattern structure may be modified, by varying the extent of overlaps and substrate rotation.

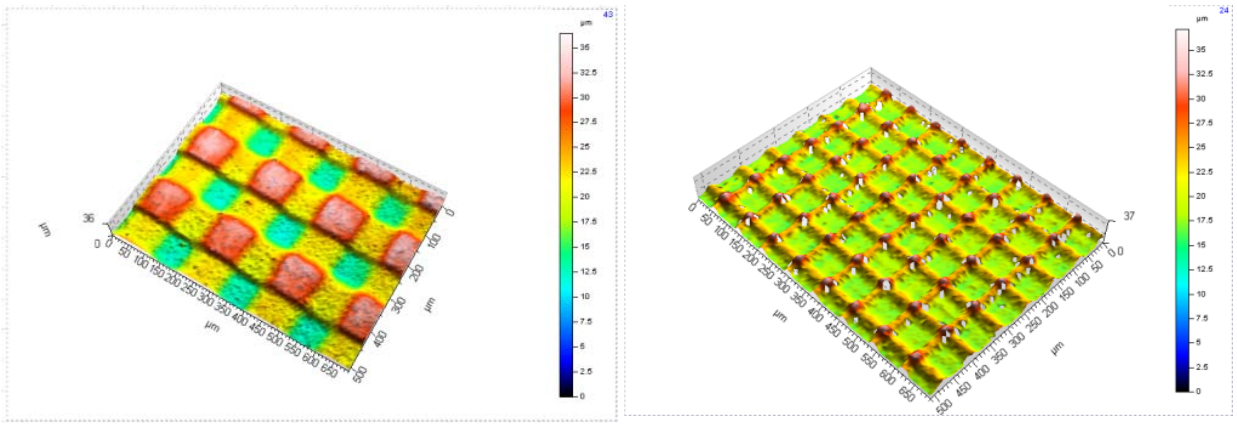

Figure 2. Areal view of micro pattern structures machined using a square mask

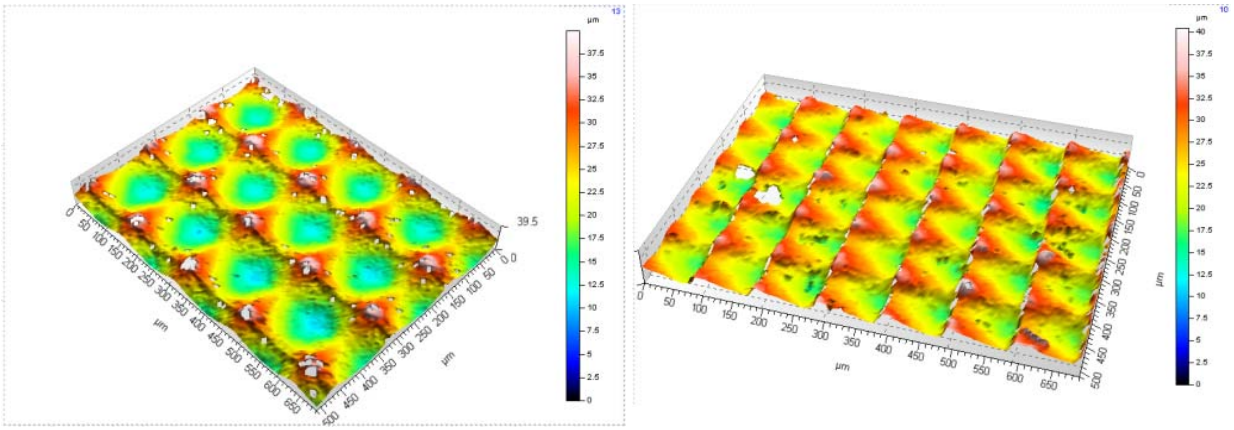

Figure 3. Areal view of micro pattern structures machined using a triangular mask

Thermal shock from the laser photo-thermal process causes micro-cracking of the glass substrate, and these cracks are typically subsurface and do not contribute to the surface topography. The micro-cracks will act as fatigue crack initiation sites if the glass substrate is subject to cyclic stress reversals, causing premature failure of the substrate. Previous work [3,4] implemented an annealing heat treatment process to heal the micro-cracks, but this technique has not been implemented in this research because it is an unnecessary process within the current research at this point in time.

4 ELECTROLESS COPPER PLATING OF GLASS

Electroless plating (auto-catalytic plating) of the glass is necessary because the glass substrate is non-conductive and therefore not suitable for traditional electroplating techniques. Typical electroless copper plating procedures include substrate cleaning, catalyst dipping and copper bath dipping. Electroless deposition is a self-accelerating process in which metal ions are chemically reduced at catalytic surface substrates. The specific processes used for this research are illustrated in figure 4 and can be summarized as follows:

- substrate cleaning with Decon 90 surface active cleaning agent at 60°C, for ten minutes followed by water wash;
- pretreatment dip using (3-aminopropyl) trimethoxysilane (APTS) to form a self-assembled monolayer (SAM) on the glass substrate to change the chemical functionality of the surface;
- Circuposit™ catalyst 3344/4444 to prepare the pretreated glass surface'
- final dip of the treated glass substrates in agitated Circuposit™ 3350-1 at elevated temperature (typically 45 °C); and
- final wash and dry.

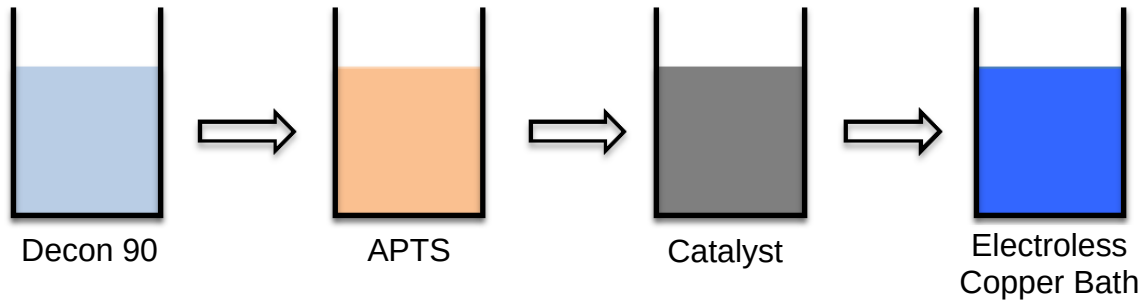

Figure 4. Electroless copper plating procedure for CMG glass

Process variables investigated included wash times, wash conditions, APTS and catalyst concentrations, solution temperatures, rate of agitation and dip times. Examples of efficacy and thickness of coating are illustrated in figure 5, showing increasing plating coverage and thickness as a function of time. Final plating experimental procedure was established and is identified in table 1. Typical copper plating thickness on all glass samples was approximately 0.5 μm. Examples of copper plating on laser machined glass patches are shown in figure 6, with copper firmly adhered on the machined substrate regions and copper typically not adhering to the non-machined substrate.

Initial experimentation resulted in machined areas of 40 mm × 10 mm (first two samples), but this was later reduced to machined areas of 10 mm × 10 mm (third sample). Furthermore, electroless chemical process improvement resulted in samples with minimal copper plating of smooth glass, as evidenced by the three samples in figure 6.

Table 1. Experimental procedure for electroless copper plating on CMG glass

Step	Process	Solution	Time	Temperature
1	Cleaning	Decon 90	5 minutes	60 °C
2	Rinse	Deionised water	3 – 5 minutes	Room temperature
3	SAM deposition	APTS ($5x10^{-3}$ mol l^{-1}) Solvent: methanol (95%)	1 hour	Room temperature
4	Rinse	Deionised water	3 – 5 minutes	Room temperature
5	Catalyst	Circuposit 3344	5 minutes	36 °C
6	Rinse	Deionised water	3 – 5 minutes	Room temperature
7	Electroless copper	Circuposit 3350-1	15 minutes	46 °C
8	Rinse and dry	Deionised water	10 minutes	Room temperature

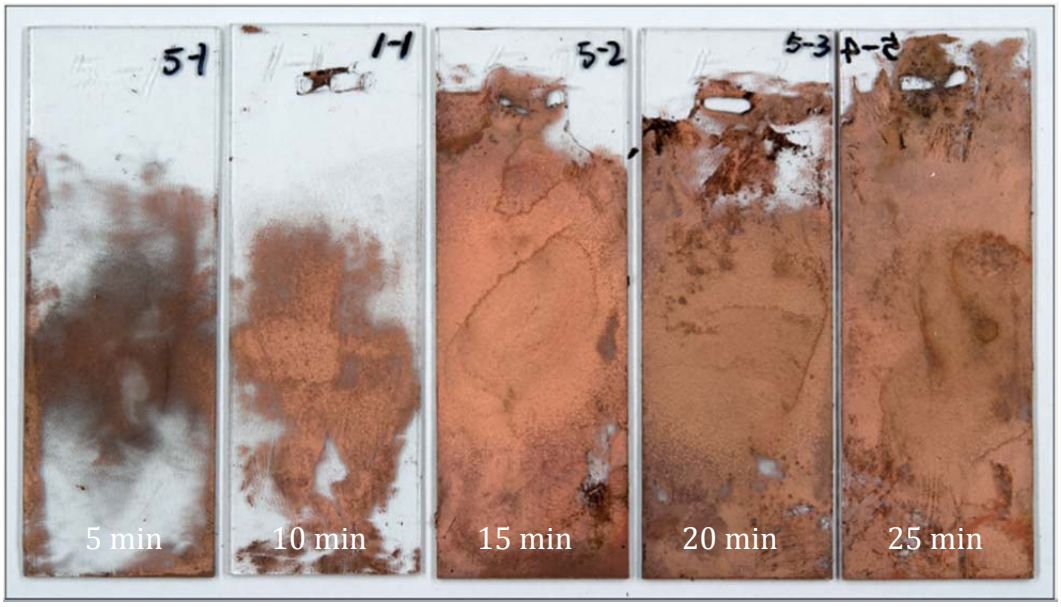

Figure 5. Electroless copper plating quality as a function of dip time

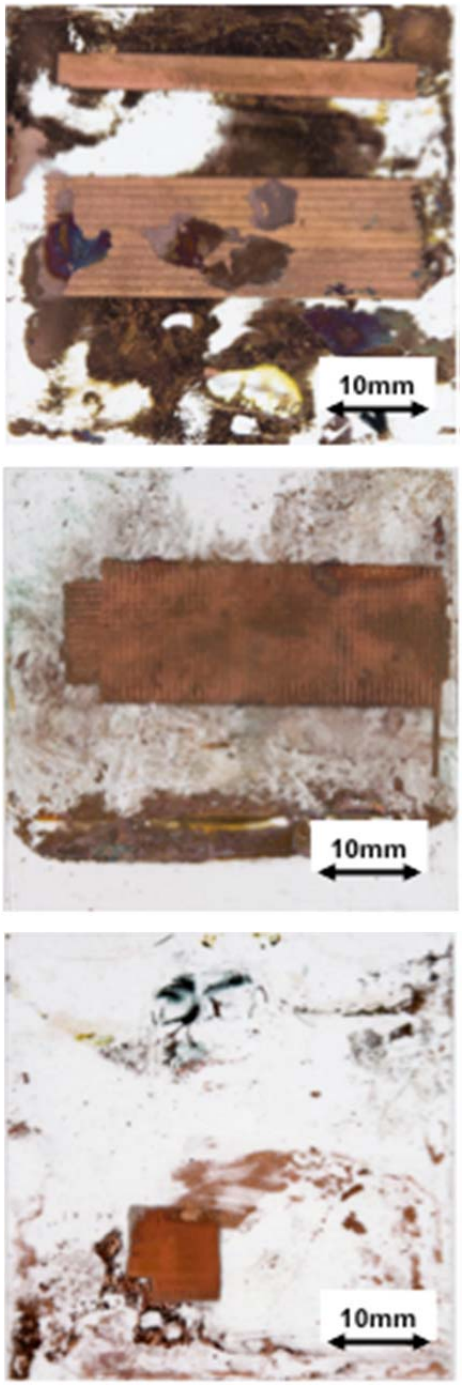

Figure 6. Examples of electroless copper plating on excimer machined CMG glass

5 SCRATCH TESTING OF GLASS

Scratch testing was chosen as the most effective quantitative assessment of adhesion strength between copper coating and the CMG glass substrates. The technique involves a diamond stylus being loaded against the sample and then drawn across the surface to cause a scratch. The load applied to the stylus is either held constant or linearly increased. Scratches can be single or multi pass. Coating failure is defined at the point where surface defects are visually identified, although failure point identification can be subjective and prone to uncertainty.

Existing researchers have demonstrated correlation of coating adhesion measurement (by scratch testing) with adhesive bond strength, through a number of proposed failure models [50-53]. Figure 7 illustrates the typical failure elements found during coating delamination, cracking, spalling, coating detachment and coating penetration/delamination.

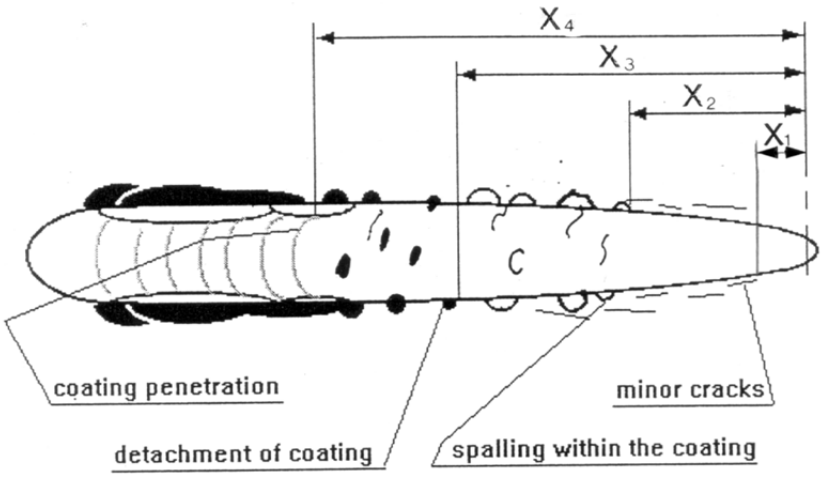

Figure 7. Different types of damage that may be observed in scratch testing [50]

This research used the ST 3001 test system at NPL which incorporates a 200 μm Rockwell C diamond stylus. Ramp loading was increased from a minimum load of 1 N to a maximum load 15 N incrementing in thirty steps. As a consequence of the scratch test result, knowledge of the sample stress state leading to delamination failure is available through direct measurement of the distance from the loading start point to coating penetration point and by theoretical calculation. Examples of test scratches on copper coated glass samples can be seen in figure 8 (optical coordinate measuring machine (CMM) images) and figure 9 (scanning electron microscope (SEM) images).

Failure points along the scratch are typically distinguished by backlighting penetrating through the copper layer and are easier to recognize using white light techniques compared to SEM images. Recognition of different failure modes may change depending on eventual copper/glass use and manufacturer. Failure was initially identified as the point of first observable failure (any mode as defined in figure 7).

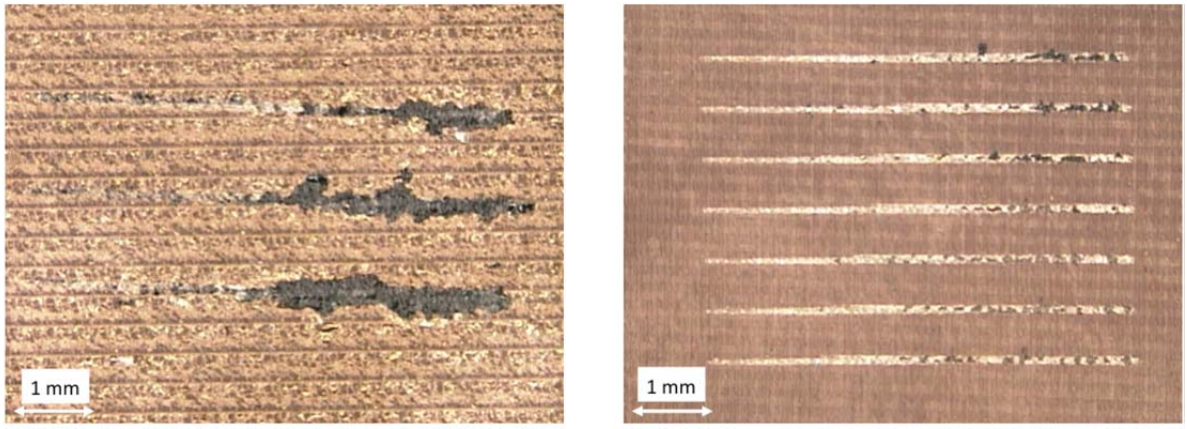

Figure 8. Optical CMM images for scratches of copper coating on CMG glass

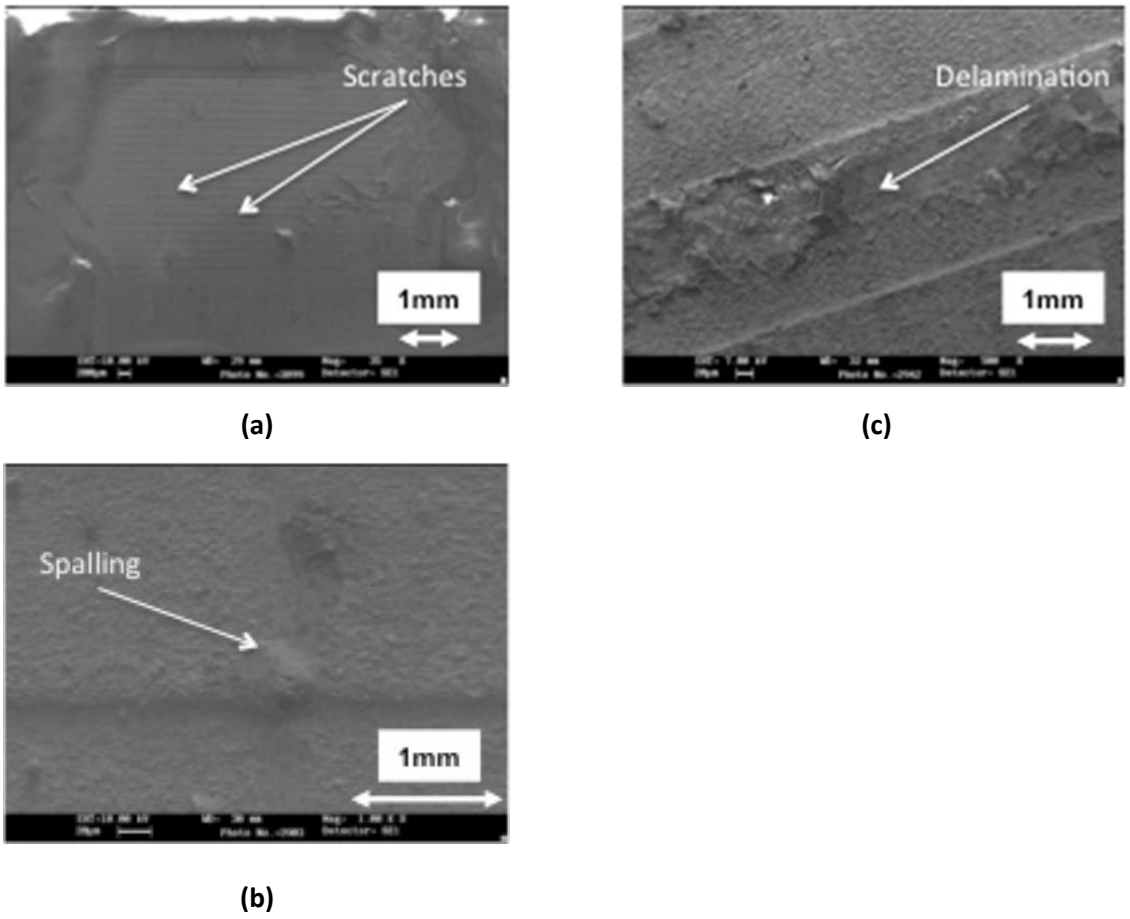

Figure 9. SEM images of scratches on copper coating on CMG glass (a) overall scratches (b) spalling position (c) delamination position

Damage patterns on the surface are correlated with acoustic emission and friction forces from the ST 3001 test system, to derive the critical loads at which various failure mechanisms occur. Graphical representation of the experimental data provides an alternative direct method of identifying the critical load of coating delamination, as shown in figure 10. Point (a) on the graph identifies the probable point of copper delamination.

Other graphical scratch testing results do not provide definitive changes and require visual analysis to identify the points of failure. Furthermore, the graphical analysis in figure 10 does not allow for the identification of the three failure criterion as defined above in figure 7.

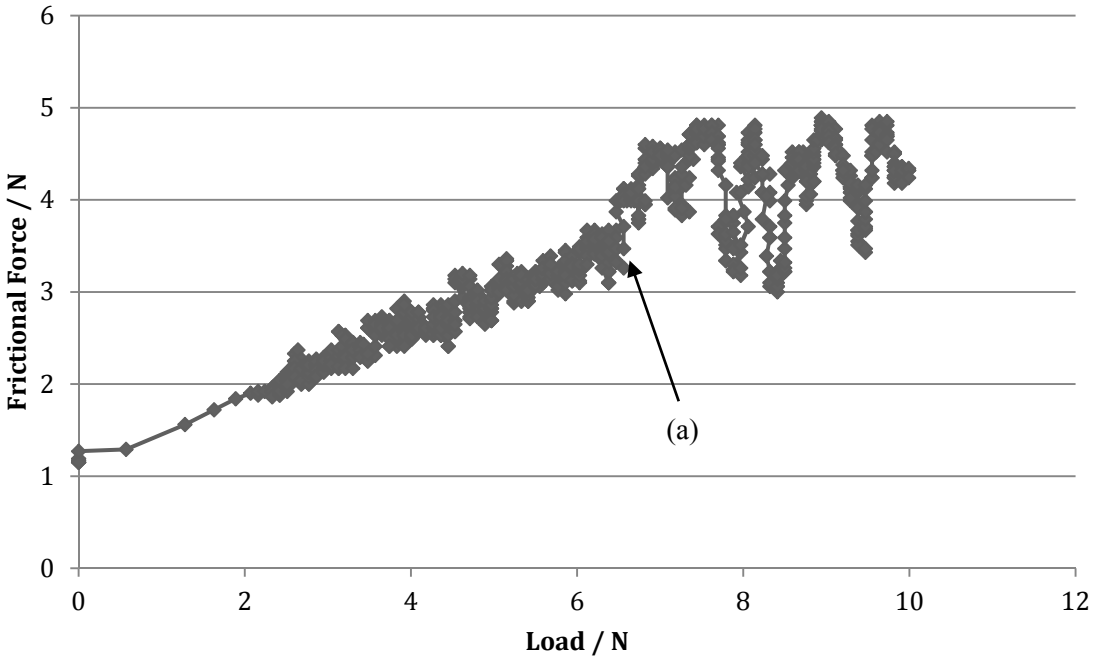

Figure 10. Scratch test result of CMG glass with structured surface

The testing of adhesive bond strength is however susceptible to a number of interfering factors that should be controlled as much as possible, for instance:

- copper coating quality (variation of thickness) affects the scratch testing result;
- coating failure occurs easily on weak and thin coated area;
- preferential failure occurs at sharp discontinuities of the glass surface (stress concentrations), that may not be representative of the bulk adhesion;
- identification of spalling and delamination is subjective and prone to human error; and
- graphical analysis (example in figure 10) does not necessarily allow for different failure modes to be identified.

6 CORRELATION OF AREAL PARAMETERS WITH CRITICAL LOAD

The research described in this report has now entered the final stage of developing causal links between critical load data and areal parameter types/values. This stage of the research is anticipated to last until mid-2012, based upon sequential batches of machined/plated CMG glass, with scratch testing completed on a three monthly basis at NPL. Each batch of glass will explore different aspects of surface texture and structure, relating this to copper adhesive bond strength.

As identified in section 3, a Zygo NewView 5000 CSI system was used to measure the surface topography of each machined micro-pattern, with consistent lens and magnification settings (10×) and field of view (700 μm × 500 μm). Surface topography and areal parameters were generated and analysed using Talymap v5.1 (DigitalSurf) surface texture processing software that is designed to be compliant with ISO 25178-2 [11]. Filtering of the data initially considered a consistent and fixed set of wavelength cut-off values (typically 80 μm). However, the use of standard filter parameters for all glass samples did not allow appropriate differentiation between micro-roughness components and structural components of the glass, leading to subsequently limited correlation with critical load.

Re-evaluation of the laser machined surfaces identified three scenarios that exist which required clarification and quantification:

- the correlation between the micro-roughness component of the glass surface and the critical load;
- the correlation between the structural component of the glass surface and the critical load; and
- the correlation between the micro-roughness and structural components of the glass surface and the critical load.

Micro-roughness on the glass surface is an inherent function of the stochastic nature of the excimer laser wavefront spatial characteristics (section 3), and has been evaluated in its own right with glass samples featuring micro-roughness, but no structure.

Furthermore, process consideration of this data (and other data sets) confirmed the requirement to investigate a number of potential failure modes for data processing investigation, because the failure mode analysis is prone to premature and/or random copper bond failure, which is illustrated in the two sets of tracks in figure 8 (black points along the scratches indicate possible localized failure points). This is typified by a scratch testing stylus impacting on a structural discontinuity, causing a localized stress concentration resulting in localized failure that is not indicative of bulk bond strength and is illustrated in figure 11.

Alignment of the scratch testing stylus with the sample is a manual process and therefore difficult to guarantee alignment with the preferential direction of the structured surface. Figure 11 shows slight misalignment of the scratch track causing a prolonged impact on a structure edge along each track. (half way along each track – seen as a black line across the scratch). Once the stylus leaves the feature edge and continues along the structure surface, plating failure is no longer observed, until the stylus load reaches the critical value at the end of each scratch. Failure at this point is again indicated by long dark elements on the scratch.

Figure 11. Premature plating failure as a function of stylus/discontinuity impact

Consequently, analysis of the data has led to the development of three failure modes as being more representative of bulk copper adhesion (and potential user application scenarios):

- Mode 1 - simple - the point where the first failure occurs on the plated surface (as illustrated in figure 11);
- Mode 2 - consecutive - the point where three consecutive observable individual failure points are identified within a predefined length of 0.5 mm (typically a higher critical load compared to the first definition); and
- Mode 3 - continuous - the point where continuous delamination occurs for a minimum length of 0.2 mm (typically the highest critical load compared to the first two definitions).

Areal parameters (including field and feature parameters) for samples typical of those shown in figure 2 and figure 3 were calculated according to ISO 25178-2 [11]. Two correlation coefficients have been employed to quantify the strength of relationship between the areal parameter values and the mean critical load value.

- Pearson product moment correlation coefficient (ρ). This coefficient provides a measure of the strength of the linear dependence between two variables, giving a value between +1.0 and -1.0.
- Spearman's rank correlation coefficient (r). This coefficient provides a non-parametric measure of the statistical dependence between two variables, varying from -1.0 to +1.0 and does not require a linear dependence between the two variables.

In this manner, it has been possible to categorize each areal parameter in terms of the strength of correlation with the critical load values, being mindful of the definition and relevance of each parameter. In each analysis case, the quality of correlation has increased as the failure mode has been changed from simple, to consecutive, to continuous. Table 2 shows correlation values for four parameters that have demonstrated the strongest behavioural relationships with the copper/glass critical load values.

Table 2. Areal parameters and associated correlation coefficient values

Areal Parameter	Spearman Coefficient Value (r)	Pearson Coefficient value (ρ)
Spc	-0.86	-0.81
Sq	-0.81	-0.76
Vvc	-0.80	-0.75
Sdq	-0.77	-0.73

These parameters have been identified as having potential for appropriately describing the glass surfaces in the context of bonding, on the basis of the correlations results within the data sets, but also with reference to their descriptions and mathematical functions as identified in ISO 25178-2 and other sources [54 - 56]:

- *Sq* is the root mean square height of the scale limited surface, and has direct analogies to the profile *R* and *W* two dimensional line profile derived parameters [10]. As one of the height parameters, its value depends on height deviation of the surface and is one of the most general of the areal parameters available.

- *Spc* is arithmetic mean peak curvature and is one of a number feature parameters which directly consider and quantify the influence of surface features (hills, dales saddle points, ridge lines and course lines), as a function of surface segmentation and filtration.

- *Sdq* is the root mean square gradient of the scale limited surface within the definition area, and is a hybrid parameter that is generated on the basis of amplitude and spatial information about the surface. Note that *Sdq* is a dimensionless parameter.

- *Vvc* is the core void volume of the scale limited surface. This is one of a number of material/void volume parameters derived from the volume information of the areal material ratio curves, with the *Vvc* parameter functionally related to the 10 % to 80 % range of the material ratio.

Individual graphs are presented in figures 12 to 15 and illustrate the initial relationships between critical load from the scratch testing results and the specific areal parameters. These data are based on the failure modes identified above, with each mode plotted for each areal parameter.

In all four cases, strong trends have been identified between critical load and the respective areal parameter, although the *Vvc* and *Sq* parameters are showing more scatter as the areal value increases. In comparison, the *Spc* and *Sdq* parameters are showing very little scatter with the exception of the 5 N critical load value data point in each case. It should be noted that the maximum load applied by the scratch testing equipment was 15 N, this force being determined by the failure of the glass substrate at greater loads. If no copper plating failure is observed during a scratch test, then the default critical load value will be 15 N. Consequently, it is possible that some of the copper/glass samples may have higher bond strengths than 15 N, but it has not been possible to quantify this strength. However, it is recognized that there is a need to reinforce these graphical and numerical comparisons with further data points from additional copper plated glass samples.

Analysis of failure modes 1 and 2, shows that there are no significant correlations between areal value and critical load. This is not surprising because the definitions of these two failure modes are susceptible to spurious, non-representative plating failure as a function of edge effect stress concentrations in the case of mode 1, and localized random defects in the case of mode 2. This fact reinforces the decision to regard failure mode 3 as the most rigorous and consistent test for copper plating failure (and therefore adhesive bond strength).

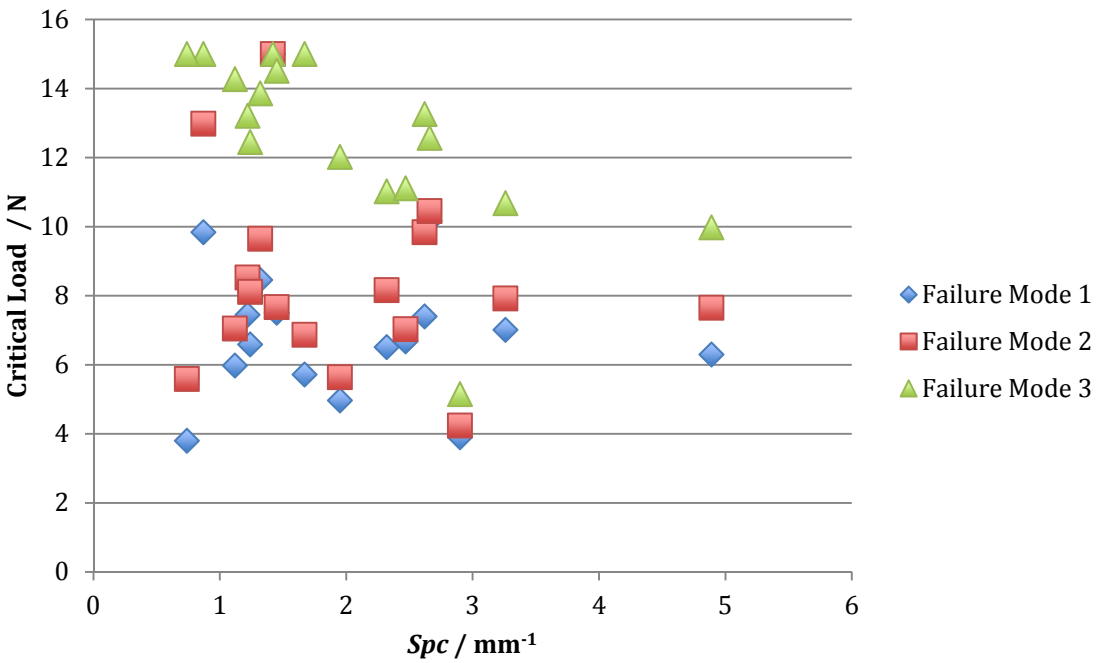

Figure 12. *Spc* parameter value as a function of critical load and failure mode (r = -0.86, ρ = -0.81)

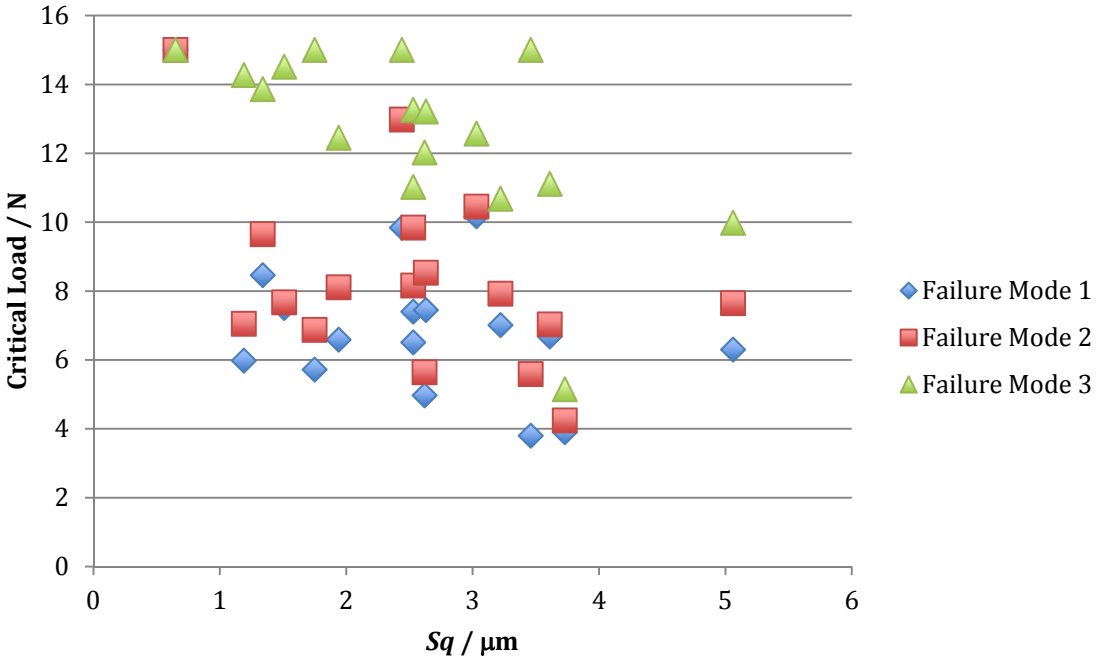

Figure 13. *Sq* parameter value as a function of critical load and failure mode (r = -0.81, ρ = -0.76)

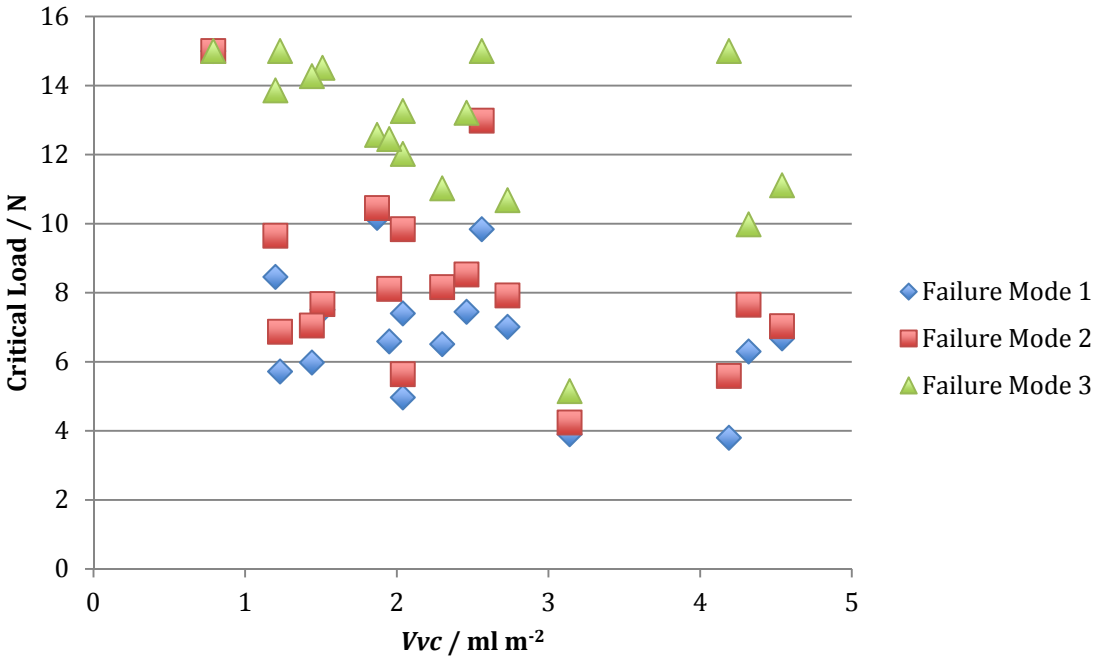

Figure 14. *Vvc* parameter value as a function of critical load and failure mode (r = -0.80, ρ = -0.75)

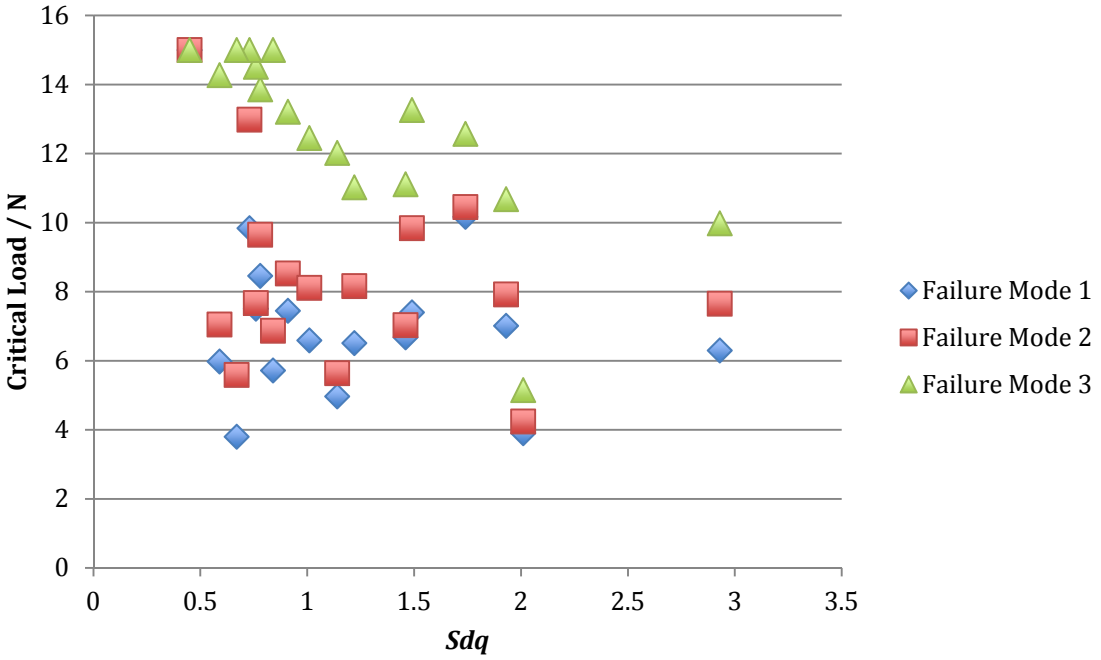

Figure 15. *Sdq* parameter value as a function of critical load and failure mode (r = -0.77, ρ = -0.73)

7 CONCLUSIONS AND FURTHER WORK

The research presented here identifies the role that surface topography may have on influencing the mechanical bond strength of the electroless copper plating on glass substrates. This process is being achieved *via* controlled excimer based laser based machining of glass, areal parameterization of the surfaces, electroless copper plating, critical failure mode identification using scratch testing, and finally correlation / statistical analysis of critical load to areal parameter. Current achievements and conclusions of this work are listed below.

- Novel and bespoke structured geometries have been machined onto CMG glass substrates using controlled excimer laser ablation, with a variety of mask geometries, mask dimensions, laser parameter settings.

- Geometry structure has ranged laterally from 20 μm to 100 μm, with typical feature depths of between 5 μm and 10 μm.

- Areal data sets have been produced, typically using CSI techniques, with ISO 25178-2 areal parameters being identified and produced for different glass structures.

- Copper has been deposited onto machined CMG glass surfaces to form interconnection tracks by electroless copper plating. Optimal copper plating parameters such as substrate cleaning, process temperatures, solution concentration, agitation characteristics and dipping time have been identified.

- Scratch testing techniques have been implemented to quantify adhesive bond strength of the copper plating, leading to the identification of critical loads.

- Visual comparisons and numerical correlation comparisons have been completed on current data, initially identifying four ISO 25178-2 areal parameters of interest (*Sdq, Spc, Sq, Vvc*). These areal parameters have shown strong correlations (in the range of 73 % to 86 %) between parameter values and critical load values (adhesive bond strength), causing further consideration with respect to failure mode type and data filtering strategies.

- Publications have been produced or have been submitted for review [57 - 59] disseminating the results of the initial work.

This research is on-going with five months of project time still to be invested in various aspects of the work. The future priorities are summarized below.

- Further excimer laser machining will focus on producing smaller depth of the surface structure, and small pitch of features. This work will allow more data to be input into the correlation analysis of the existing areal parameter investigation. Additional scratch testing is to be completed at NPL.

- Coating thickness measurements and scratch adhesion models will be further investigated and implemented (where relevant).

- Filter parameters will be investigated (where relevant) to consider three different scenarios of relationship between micro-roughness/structural components and the critical load / bond failure mechanism.

- Journal papers and a PhD Thesis will be produced to further disseminate the results of the later stages of the research.

8 ACKNOWLEDGEMENT

This research is a collaboration between Loughborough University (UK) and the UK National Physical Laboratory. The research has been part funded by the EPSRC 3D-Mintegration Grand Challenge project, the Wolfson School of Mechanical & Manufacturing Engineering, and the 2008 to 2011 NMO Engineering & Flow Metrology Programme. The authors would also like to thank Qioptiq Ltd for the supply of CMG glass.

9 REFERENCES

[1] Schröder H, Arndt-Staufenbiel N, Cygon M, Scheel W 2003 Planar glass waveguides for high performance Electrical-Optical-Circuit Boards (EOCB) - The glass layer concept *Proceedings of the 53rd Electronic Components and Technology Conf, New Orleans, May* 1053-1059

[2] Cui X, Hutt D A, Conway P P 2008 An investigation of electroless copper films deposited on glass Proc. 2nd IEEE Electronics System-Integration Technology Conf, London, Sep 105 -110

[3] Cui X, Bhatt D, Khoshnaw F M, Hutt D A, Conway P P 2008 Glass as a substrate for high density electrical interconnect Proc. 10th Int. IEEE Electronics Packaging Technology Conf, Singapore, Dec 12 -17

[4] Bhatt D 2009 Excimer laser machining of glass for high density substrate manufacture (Loughborough University, PhD Thesis)

[5] Cui X 2009 Electroless metallization of glass for electrical interconnect (Loughborough University, PhD Thesis)

[6] Khoshnaw F M H 2010 Glass multilayer bonding for high density interconnect (Loughborough University, PhD Thesis)

[7] Baburaj E G, Starikov D, Evans J, Shafeev G A, Bensaoula A 2007 Enhancement of adhesive joint strength by laser surface modification International Journal of Adhesion & Adhesives 27 268-276

[8] Zhang X M, Yue T M, Man H C 1997 Enhancement of ceramic-to-metal adhesive bonding by excimer laser surface treatment Materials Lett. 30 327-332

[9] Starikov D, Boney C, Pillai R, Bensaoula A, Shafeev G A, Simakin A V 2004 Spectral and surface analysis of heated micro-column arrays fabricated by laser-assisted surface modification Infrared Physics & Technology 45 159–167

[10] Leach R K 2001 The measurement of surface texture using stylus instruments NPL Measurement Good Practice Guide No. 37

[11] ISO 25178-2 2012 Geometrical product specifications (GPS) - Surface texture: Areal - Part 2: Terms, definitions and surface texture parameters (International Organization for Standardization)

[12] Stout K J, Sullivan P J 1992 The use of 3-D topographic analysis to determine the micro-geometric transfer characteristics of textured sheet surfaces through rolling Ann. CIRP 41 621-624

[13] Wennerberg A, Ohlssont R, Rosknt B G, Andersson B 1996 Characterizing three-dimensional topography of engineering and biomaterial surfaces by confocal laser scanning and stylus techniques Medical Engineering Physics 18 548-556

[14] Xie H C, Chen D R, Kong X M 1999 An analysis of the three-dimensional surface topography of textured cold-rolled steel sheets Tribology International 32 83-87

[15] Jiang X Q, Blunt L, Stout K J 1999 Three-dimensional surface characterization for orthopaedic joint prostheses Journal of Engineering in Medicine 213 49-68

[16] Ramasawmy H, Blunt L 2002 3D surface topography assessment of the effect of different electrolytes during electrochemical polishing of EDM surfaces International Journal Of Machine Tools and Manufacture 42 567-574

[17] Ramasawmy H, Blunt L, Rajurkar K P 2005 Investigation of the relationship between the white layer thickness and 3D surface texture parameters in the die sinking EDM process Prec. Eng. 29 479-490

[18] Butler D L, Blunt L A, See B K, Webster J A, Stout K J 2002 The characterisation of grinding wheels using 3D surface measurement techniques Journal of Materials Processing Technology 127 234–237

[19] Al-Nawas B, Götz H 2003 Three-dimensional topographic and metrologic evaluation of dental implants by Confocal Laser Scanning Microscopy Clinical Implant Dentistry And Related Research 5 176-183

[20] Suh A Y, Polycarpou A A, Conry T F 2003 Detailed surface roughness characterization of engineering surfaces undergoing tribological testing leading to scuffing Wear 255 556-568

[21] Bénard Q, Fois M, Grisel M 2005 Influence of fibre reinforcement and peel ply surface treatment towards adhesion of composite surface International Journal of Adhesion and Adhesives 24 404–409

[22] Kundrak J, Osanna P H, Afjehi-Sada A, Bana V, 2006 Surface quality of hard turned bore holes Metrology for a Sustainable Development 17-22

[23] Krzyzak Z, Pawlus P 2006 Zero-wear of piston skirt surface topography Wear 260 554-561

[24] Senin N, Ziliotti M, Groppetti R 2007 Three-dimensional surface topography segmentation through clustering Wear 262 395-410

[25] Sul Y T, Kang B S, Johansson C, Um H S, Park C J, Albrektsson T 2009 The roles of surface chemistry and topography in the strength and rate of oseointegration of titanium implants in bone Journal of Biomedical Materials Research A89 942-950

[26] Ávila R F, Godoy C, Abrão A M, Lima M M 2008 Topographic analysis of the crater wear on TiN, Ti(C, N) and (Ti, Al)N coated carbide tools Wear 265 49-56

[27] Michalski J 2009 Surface topography of the cylindrical gear tooth flanks after machining International Journal of Advanced Manufacturing Technology 43 513-516

[28] Waikar R A, Guo Y B 2008 A comprehensive characterization of 3D surface topography induced by hard turning versus grinding Journal of Materials Processing Technology 197 189-199

[29] Nguyen A T, Butler A 2008 Correlation of grinding wheel topography and grinding performance: A study from a viewpoint of three-dimensional surface characterisation Journal of Materials Processing Technology 208 14-23

[30] Scardino A J, Hudleston D, Peng Z, Paul N A, de Nys R 2009 Biomimetic characterisation of key surface parameters for the development of fouling resistant materials Biofouling 25 83-93

[31] Takadoum J,Houmid Bennani H 1997 Influence of substrate roughness and coating thickness on adhesion, friction and wear of TiN films Surface and Coatings Technology 96 272-282

[32] Hallab N J, Bundy K J, O'Connor K, Moses R L, Jacobs J J 2001 Evaluation of metallic and polymeric biomaterial surface energy and surface roughness characteristics for directed cell adhesion Tissue Engineering 7 55-71

[33] Shahid M, Hashim S A 2002 Effect of surface roughness on the strength of cleavage joints International Journal of Adhesion and Adhesives 22 235–244

[34] Chong E K, Stevens M G, Nissen K E 2003 Effect of surface roughness on the adhesion of electrolessly plated platinum to poly (ethylene terephthalate) films Journal of Adhesion 79 667-681

[35] Garbacz A, Courard L, Kostana, K 2006 Characterization of concrete surface roughness and its relation to adhesion in repair systems Materials Characterization 56 281-289

[36] Bénard Q, Fois M, Grisel M 2006 Surface treatment of carbon/epoxy and glass/epoxy composites with an excimer laser beam International Journal of Adhesion and Adhesives 26 543–549

[37] Minaki K, Kitajima K, Minaki K, Izawa M, Tosha K 2005 Improvement of surface texture of stainless steel by utilizing dry blasting - 2nd report: Effect of blasting conditions on wettability Key Engineering Materials 291-292 265-270

[38] Minaki K, Kitajima K, Minaki K, Izawa M, Tosha K 2007 Improvement of surface texture of stainless steel by utilizing dry blasting - 3rd report: Effect of blasting surface texture on adhesion of plating Key Engineering Materials 329 353-358

[39] Menezes P L, Kishore A, Kailas S V 2006 Studies on friction and transfer layer: role of surface texture Tribology Letters 24 265-273

[40] Jiang Z X, Huang Y D, Liu L, Long J 2007 Effects of roughness on interfacial performances of silica glass and non-polar polyarylacetylene resin composites Applied Surface Science 253 9357-9364

[41] Zappone B, Rosenberg K J, Israelachvili, J 2007 Role of nanometer roughness on the adhesion and friction of a rough polymer surface and a molecularly smooth mica surface Tribology Letters 26 191-201

[42] Novák I, Sysel P, Zemek J, Špírková M, Velić D, Aranyosiová M, Florián Š, Pollák V, Kleinová A, Lednickỳ F, Janigová I 2009 Surface and adhesion properties of poly (imide-siloxane) block copolymers European Polymer Journal 45 57-69

[43] Indolfi L, Causa F, Netti P A 2009 Coating process and early stage adhesion evaluation of poly(2-hydroxy-ethyl-methacrylate) hydrogel coating of 316L steel surface for stent applications Journal of Material Science: Materials in Medicine 20 1541-1551

[44] Ayrilmis N, Winandy J E 2009 Effects of post heat-treatment on surface characteristics and adhesive bonding performance of medium density fiberboard Materials and Manufacturing Processes 24 594-599

[45] Hecht J 1992 The laser guidebook 2nd Edition (McGraw-Hill, New York)

[46] Tseng A A 2007 Recent developments in micromachining of fused silica and quartz using excimer lasers Physica Status Solidi A204 709–729

[47] Petzing J, Coupland J M, Leach R K 2010 The measurement of rough surface topography using coherence scanning interferometry NPL Measurement Good Practice Guide No. 116

[48] BS EN ISO 25178-6 2010 Geometrical product specifications (GPS) - Surface texture: Areal, Part 6: Classification of methods for measuring surface texture (International Organization for Standardization)

[49] Leach R K 2010 Fundamental principles of engineering nanometrology (Elsevier: Amsterdam)

[50] Maxwell A S 2001 Review of test methods for coating adhesion NPL Report MATC (A) 49

[51] Bull S J, Berasetegui E G 2006 An overview of the potential of quantitative coating adhesion measurement by scratch testing Tribology International 99–114

[52] Bull S J 1991 Failure modes in scratch adhesion testing Surface and Coatings Technology 25-32

[53] Chalker P R, Bull S J, Rickerby D S 1991 A review of the methods for the evaluation of coating-substrate adhesion Proc. 2nd International Conference on Plasma Surface Engineering, Garmisch-Partenkirchen, Sep 583-592

[54] Stout K J, Blunt L A 2003 Three dimensional surface topography (Penton Press)

[55] Blunt L A, Jiang X 2003 Advanced techniques for assessment surface topography (Kogan Page Science)

[56] Scott P J 2004 Pattern analysis and metrology: the extraction of stable features from observable measurements Proc. Roy. Soc. A460 2845-2864

[57] He B, Webb P, Petzing P N, Conway P 2011 The use of areal parameters to improve electroless copper plating bond strength on glass substrates Proc. 13th International Conference on Metrology and Properties of Engineering Surfaces, Twickenham, UK, April

[58] He B, Webb P, Petzing J N, Conway P 2011 Improving plated copper adhesion for metallisation of glass PCBs Proc. 12th International Conference on Electronic Packaging Technology & High Density Packaging (ICEPT-HDP2011), Shanghai, China 284 – 288

[59] He B, Petzing J N, Webb P, Conway P, Leach R K 2012 The assessment of areal surface texture parameters for characterizing the adhesive bond strength of copper plated micro-machined glass, Abstract submitted October 2011 for the 12th euspen International Conference, Stockholm, June 2012.

APPENDIX 1

Table 3. Example publications on the application of areal parameters

People	Year	Application area	Parameters used	Ref.
Stout and Sullivan.	1991	Sheet surfaces through rolling	*Sa Sq Ssk Sku*	12
Wennerberg *et al.*	1995	Engineering and biomaterial surfaces	*Sa Sq Sz Ssk Sku Sk Spk Svk Sr1 Sr2*	13
Xie *et al.*	1999	Cold-rolled steel sheet	*Sq Sds*	14
Jiang, Blunt and Stout.	1999	Bio-engineering	*Sq Sz Ssk Sku Sds Str Sal Std SΔq Ssc Sdr Sbi Sci Svi*	15
Ramasawmy and Blunt.	2001 2005	Electrochemical polishing surfaces and white layer thickness in EDM	*Sq Sz Sds Sm Sc Sv Sa S5z*	16,17
Butler *et al.*	2002	Grinding wheels	*Sds Ssc Sq*	18
Al-Nawas and Götz.	2003	Dental implants	*Sa Sdr*	19
Suh *et al.*	2003	Wear conditions of discs and steel pins	*Sa Sq Sz Ssk Sku Sds Str Std SΔq Ssc Sdr Sbi Sci Svi*	20
Bénard *et al.*	2005	Adhesion of composites	*Sa*	21
Kundrak *et al*.	2006	Hard turned bore holes	*Sa Sq Sz Ssk Sku Sds Str Std Sal SΔq Ssc Sdr Sbi Sci Svi*	22
Krzyzak and Pawlus.	2006	Piston skirts	*Sq Ssk Str S Δq St±3σ Sku, Sds, SSc*	23
Senin *et al.*	2006	Segmentation through clustering	*Sa Sq Sz Ssk Sku Sds Str Std SΔq Ssc Sdr Sbi Sci Svi*	24
Sul *et al.*	2007	Titanium implants in bone	*Sa Sdr Sds*	25
Avila *et al.*	2008	The crater wear in coated hard metal tools	*Sa Sq Sk Svk Spk Ssk Sku*	26
Michalski.	2008	The cylindrical gear tooth flanks	*Sa Sq……*	27
Waikar and Guo.	2008	Turned and ground surfaces	*Sa Sq Sp Sv St Sz Ssk Sku Sds Str Sal Std SΔq Ssc Sdr STp Smmr Smvr*	28
Nguyen and Butler	2008	Grinding wheel topography	*Sds Ssc Sq Sal*	29
Scardino *et al.*	2009	Antifouling technology	*Sa Ssk Str*	30

Table 4. Development of characterisation surface texture for adhesion

People	Year	Material	Methods	Parameter used	Ref.
Takadoum and Bennani	1997	TiN deposited on steel substrate	Reactive ion plating Scratch tests	*Ra*	31
Hallab *et al.*	2001	Metallic and polymeric biomaterial	Shear strength test	*Ra*	32
Shahid and Hashim	2002	Cleavage joint strength	Tensile destructive test	*Ra*	33
Chong *et al*.	2003	Plated platinum to poly(ethylene terephthalate) films	Electroless plating Tape testing.	*Rq*	34
Garbacz *et al*.	2005	Concrete	Pull-off test	*Ra*	35
Bénard *et al.*	2006	Gass/epoxy and carbon/epoxy composites	Shear test	*Sa*	36
Minaki *et al.*	2005 2007	Plating of martensitic stainless steel	Scratch test	*Ra*	37, 38
Menezes *et al.*	2006	Ground EN8 steel flats	Scratch test	*Ra*	39
Jiang *et al.*	2007	Silica glass / polyarylacetylene resin composites	Shear test	*Ra*	40
Zappone *et al.*	2007	Polymer	Peeling test	*Rq*	41
Novák *et al.*	2008	Poly(imide-siloxane) (PIS) block copolymers	Peel test and shear test	Surface energy	42
Indolfi *et al.*	2009	Coating onto 316L steel stent	Spray-coating Pull-off test	*Ra* *Rq*	43
Ayrilmis and Winandy	2009	Adhesive bonding strength between MDF surface and veneer sheet	Delamination test	*Ra*	44